

Effects of addition of TiO₂ nanoparticles on mechanical properties and ionic conductivity of solvent-free polymer electrolytes based on porous P(VdF-HFP)/P(EO-EC) membranes

Jae-Deok Jeon, Myung-Jin Kim, Seung-Yeop Kwak*

Hyperstructured Organic Materials Research Center (HOMRC), and School of Materials Science and Engineering, Seoul National University, San 56-1, Sillim-dong, Gwanak-gu, Seoul 151-744, South Korea

Received 10 May 2006; accepted 11 August 2006

Available online 2 October 2006

Abstract

To enhance the performance (i.e., mechanical properties and ionic conductivity) of pore-filling polymer electrolytes, titanium dioxide (TiO₂) nanoparticles are added to both a porous membrane and its included viscous electrolyte, poly(ethylene oxide-*co*-ethylene carbonate) copolymer (P(EO-EC)). A porous membrane with 10 wt.% TiO₂ shows better performance (e.g., homogeneous distribution, high uptake, and good mechanical properties) than the others studied and is therefore chosen as the matrix to prepare polymer electrolytes. A maximum conductivity of $5.1 \times 10^{-5} \text{ S cm}^{-1}$ at 25 °C is obtained for a polymer electrolyte containing 1.5 wt.% TiO₂ in a viscous electrolyte, compared with $3.2 \times 10^{-5} \text{ S cm}^{-1}$ for a polymer electrolyte without TiO₂. The glass transition temperature, T_g is lowered by the addition of TiO₂ (up to 1.5 wt.% in a viscous electrolyte) due to interaction between P(EO-EC) and TiO₂, which weakens the interaction between oxide groups of the P(EO-EC) and lithium cations. The overall results indicate that the sample prepared with 10 wt.% TiO₂ for a porous membrane and 1.5 wt.% TiO₂ for a viscous electrolyte is a promising polymer electrolyte for rechargeable lithium batteries.

© 2006 Elsevier B.V. All rights reserved.

Keywords: Pore-filling polymer electrolyte; Porous membrane; TiO₂ nanoparticles; Ionic conductivity; Rechargeable lithium batteries; Conductivity

1. Introduction

Recently, an attempt has been made to combine both a gel (GPE) and a solvent-free polymer electrolyte (SPE) through the concept of pore-filling polymer electrolytes. In that procedure, instead of organic solvents, a viscous polymer complexed with LiCF₃SO₃ was filled into the pores of a porous membrane, to produce a polymer electrolyte [1,2]. The viscous polymer was poly(ethylene oxide-*co*-ethylene carbonate) copolymer (P(EO-EC)) with a low number average molecular weight of about 1800 g mol⁻¹; it was synthesized using ethylene carbonate (EC). Due to the high polarity of carbonate groups linked by ether moieties, the dielectric constant of P(EO-EC) should be higher than that of polyether-based systems [3]. An interesting feature of the P(EO-EC) is its lack of crystallinity. Therefore, the amor-

phous nature of the P(EO-EC) allows this material to be used successfully as an ion-conducting polymer electrolyte without any negative effects from crystallization. The porous membranes were composed of two materials: poly(vinylidene fluoride-*co*-hexafluoropropylene) (P(VdF-HFP)) with excellent mechanical properties and P(EO-EC) with good flexible properties. The introduction of P(EO-EC) into the membranes leads to high porosity, which could reach up to 65% depending on the P(EO-EC) composition. Despite the fact that the pore-filling polymer electrolytes show higher conductivity ($3.7 \times 10^{-5} \text{ S cm}^{-1}$ at 25 °C) than conventional SPEs, they still have some drawbacks such as deterioration of mechanical properties (due to the addition of viscous P(EO-EC)) and low conductivity for practical applications.

In recent years, many researchers have promoted the development of composite polymer electrolytes (CPEs) by introducing ceramic fillers (such as SiO₂, Al₂O₃, γ -LiAlO₂, TiO₂) [4–13], which results in improved mechanical properties, enhanced ionic conductivity, and better interfacial stability between lithium and

* Corresponding author. Tel.: +82 2 880 8365; fax: +82 2 885 1748.

E-mail address: sykwak@snu.ac.kr (S.-Y. Kwak).

the polymer electrolyte. In particular, recent studies of CPEs have tended towards the addition of nano-sized TiO_2 in polymer electrolytes. Liao and Wu [11] reported that acrylic acid grafted polyethylene-octene elastomer (POE-*g*-AA)/ TiO_2 hybrid had a positive effect on the mechanical properties of POE/ TiO_2 hybrid because the carboxylic acid groups of acrylic acid act as coordination sites for the titania phase. It was also found that the tensile strength increased up to a maximum value and then decreased with increase in TiO_2 because excess particles (e.g., greater than 10 wt.% TiO_2) caused aggregation between the organic and inorganic phases. In another study [12], it was reported that there are interactions, i.e., weak coordination bonds, between the alkylene oxide segments and TiO_2 . From these investigations, it is to be expected that porous membranes consisting of P(EO-EC), P(VdF-HFP) and TiO_2 nanoparticles will ensure greater enhancement of the mechanical properties due to interactions between the carbonate and oxide segments of P(EO-EC) and TiO_2 .

On the other hand, the addition of TiO_2 induces an improvement in the ionic conductivity of polymer electrolytes. In general, it is widely accepted that the addition of TiO_2 into semi-crystalline polymers suppresses crystallization and enlarges the amorphous phase, which result in an enhancement of ionic conductivity as shown by Chung et al. [13]. In this study, however, TiO_2 was added to the perfectly amorphous polymer, P(EO-EC). Although there have been only a few investigations conducted on the effect of TiO_2 on polymer electrolytes based on amorphous polymers, it is safe to assume that their conductivity can be enhanced because the interaction occurs between hydroxyl groups on the surface of TiO_2 and carbonate and ether groups in P(EO-EC), which eventually induces improvement in the conductivity because of the weakening of P(EO-EC) oxygen–lithium cation interactions. Recently, Liu et al. [14] reported the effect of nano-sized SiO_2 on the electrochemical properties of macro-monomers with a PEO-like structure which is a fully amorphous PEO. They achieved an increased transference number when SiO_2 , formed by in situ reaction, was added. The effect was interpreted to be the result of the formation of free volume, which was produced by the hydrogen bonds between the hydroxyl groups on SiO_2 nanoparticle surfaces and the ether groups of the PEO branches.

This study focuses on improvement of the mechanical properties and ionic conductivities of polymer electrolytes by the addition of TiO_2 nanoparticles into a porous membrane and a viscous electrolyte. The effects of the TiO_2 nanoparticles on the performance of polymer electrolytes are presented and discussed.

2. Experimental

2.1. Preparation of porous membranes and polymer electrolytes

Porous membranes prepared by a phase inversion method were composed of two materials: poly(vinylidene fluoride-co-hexafluoropropylene) (P(VdF-HFP), $M_w = 4.6 \times 10^5$, Aldrich Chemicals) with excellent mechanical properties, and

P(EO-EC) with good flexible properties. The P(EO-EC) ($M_n = 1800 \text{ g mol}^{-1}$) was synthesized by a ring-opening polymerization of EC in the presence of potassium methoxide (CH_3OK) as an initiator. The synthesis of P(EO-EC) has been described in detail in previous reports [1,2]. To prepare porous membranes with structural rigidity and high uptake of a viscous electrolyte, the weight ratio of polymers with TiO_2 (ST-01, 100% anatase, Ishihara Sangyo Kaisha), solvent (acetone), and non-solvent (triethanol amine, TEA) was optimized at 10:80:10. In previous studies, ethylene glycol (EG) was used as a non-solvent. In this study, however, TEA was chosen as a non-solvent instead of EG because of the good dispersion of TiO_2 in TEA solution, i.e., the size (ca. 60 nm) of TiO_2 nanoparticles in acetone/TEA solution ($\text{pH} \approx 10.2$) was much smaller than that (ca. 110 nm) in acetone/EG solution ($\text{pH} \approx 6.7$). As a result of the previous studies, the proportions of P(VdF-HFP) and P(EO-EC) were taken as 60 and 40 wt.%, respectively. The TiO_2 contents were varied as 0, 5, 10, 20, 30 and 40 wt.% in P(VdF-HFP)/P(EO-EC)/ TiO_2 .

First, a homogenous solution was prepared in advance by dissolving P(VdF-HFP) and P(EO-EC) in acetone at 50°C . A measured amount of TiO_2 was added to a TEA/acetone solution and then was stirred ultrasonically. Finally, the TiO_2 /acetone/TEA solution was added to a homogenous P(VdF-HFP)/P(EO-EC)/acetone solution. When a completely homogenous mixture was obtained, it was cast with a doctor blade on to a glass plate. The TEA was then removed by washing with methanol. The solvent was allowed to slowly evaporate at room temperature and then was completely removed by heating under vacuum at 50°C for 24 h, to produce a porous membrane. All porous membranes had the thicknesses of 120–160 μm .

In order to prepare the pore-filling polymer electrolyte, P(EO-EC) was first dissolved in acetone. When completely homogenous solution was obtained, appropriate amounts of lithium trifluoromethane sulfonate (LiCF_3SO_3 , Aldrich Chemicals) and TiO_2 were added. The solution was stirred further until the Li-salt became completely dissolved. The TiO_2 contents were varied as 0, 0.5, 1.0, 1.5, 2.0 and 5.0 wt.% with respect to the viscous electrolyte of P(EO-EC), LiCF_3SO_3 and TiO_2 . The resultant solution was left to evaporate the residual acetone under vacuum at room temperature. After complete evaporation of the acetone, the porous membrane was filled for several times with the heated P(EO-EC)/ LiCF_3SO_3 / TiO_2 electrolyte (also called a viscous electrolyte) by using vacuum filter equipment, thereby producing pore-filling polymer electrolytes. The mixture remaining on the surface was removed with filter paper. All procedures for preparing polymer electrolytes were carried out in a dry room.

In this study, MT_x and ET_{x-y} denote, respectively, a porous membrane containing x wt.% of TiO_2 and a polymer electrolyte filled with a viscous electrolyte containing y wt.% of TiO_2 inside the pores of the MT_x .

2.2. Characterization of porous membranes and polymer electrolytes

The thermal properties of porous membranes and the TiO_2 loading contents in porous membranes were measured by means

of a TA model 2050 TGA instrument under a nitrogen atmosphere over the temperature range 30–620 °C at a heating rate of 10 °C min⁻¹. The TiO₂ loading content, L_T , was calculated as follows:

$$L_T (\text{wt.}\%) = \frac{W_M - W_P}{W_T - W_P} \times 100 \quad (1)$$

where W_M is the total residual weight of porous membranes at 600 °C; W_P is the residual weight of polymers (i.e., MT0 consisting of P(VdF-HFP) and P(EO-EC)) at 600 °C; W_T is the residual weight of TiO₂ nanoparticles at 600 °C.

The crystalline property of porous membranes was observed with a Perkin-Elmer GX IR spectrometer in the range of 400–4000 cm⁻¹. Moreover, wide-angle X-ray diffraction (WXR) was also used to evaluate crystalline properties by using a MAC Science MXP 18A-HF X-ray diffractometer with Cu K α radiation ($\lambda = 1.5406 \text{ \AA}$), which was operated at a voltage of 40 kV and a current of 40 mA. The diffraction angle was scanned at a 2° min⁻¹ from 5° to 45°.

The uptake, U , of porous membranes was calculated by

$$U (\%) = \frac{W - W_0}{W} \times 100 \quad (2)$$

where W and W_0 are the weights of wet and dry membranes, respectively. Morphological examination of the porous membranes was made with a field-emission scanning electron microscope (FE-SEM, JEOL, JSM-6330F). The mechanical properties of porous membranes were measured at room temperature with a strain rate of 20 mm min⁻¹ according to the ASTM 882 procedure with a LLOYD LR10K universal testing instrument.

The ionic conductivity of polymer electrolytes was determined by the complex impedance technique in the temperature range of 5–95 °C and over the frequency range of 0.1 Hz–1 MHz using a Zahner Elektrik IM6 impedance analyzer. The samples for conductivity measurements were prepared by sandwiching the polymer electrolytes between two $1.7 \times 1.7 \text{ cm}^2$ stainless-steel (SS) electrodes. The ionic conductivity was obtained from the bulk resistance found in the complex impedance diagram and calculated according to the following equation:

$$\sigma = \frac{L}{R_b \times A} \quad (3)$$

where σ is the ionic conductivity; R_b is the bulk resistance of the polymer electrolyte; A is the area of the SS electrode; L is the thickness of the polymer electrolyte. Prior to measurement, each sample was allowed to equilibrate for 30 min at the given temperature. All assemblies and testing operations were performed in a dry room. The glass transition temperature, T_g , of each viscous electrolyte was determined by differential scanning calorimetry (DSC) with a TA instruments DSC 2920. About 10 mg of a given sample was sealed in a standard aluminum can and heated in a nitrogen atmosphere from -70 to 100 °C at a rate of 10 °C min⁻¹.

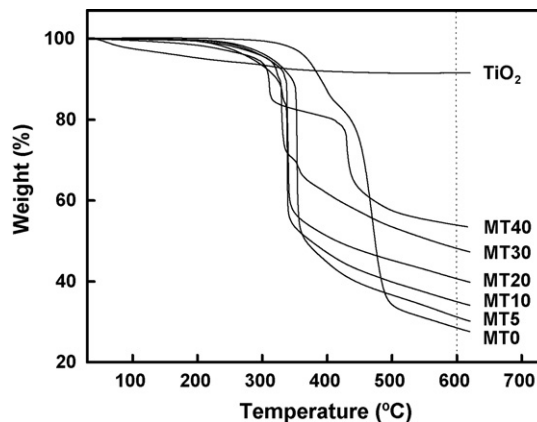


Fig. 1. Thermogravimetric curves of TiO₂ and porous membranes.

3. Results and discussion

3.1. Thermal and crystalline properties of porous membranes

The loading contents of TiO₂ nanoparticles in porous membranes were measured by thermogravimetric analysis (TGA). During manufacture of the porous membranes, they go through a course of washing with methanol to remove the non-solvent (i.e., TEA). Therefore, TGA measurements were performed to validate whether or not there was any loss of TiO₂ nanoparticles during the washing process. The residual weights of all samples were obtained at 600 °C and are shown in Fig. 1. The loading contents of TiO₂ nanoparticles in the porous membranes were calculated by using Eq. (1) and were based on the residual contents of pure polymers and pure TiO₂ nanoparticles. The data in Table 1 show clearly that there are no significant differences in the TiO₂ content between the theoretical and calculated values. This indicates that loss of TiO₂ nanoparticles does not occur during the washing process.

The thermal decomposition of TiO₂ nanoparticles and porous membranes was obtained from TGA curves (as shown in Fig. 1). The temperature at which there is a 10% weight loss (T_{d10}) of the porous membranes moves towards a lower value when TiO₂ is added. It has been generally reported [15] that the thermal stability of polymer/TiO₂ hybrid films decreases due to the evaporation of residual alcohol and physically absorbed water. Therefore, it is safe to conclude that the shift of T_{d10} of porous

Table 1
TGA parameters and uptake data of porous membranes

Sample	Loading content (wt.%) of TiO ₂ nanoparticles		T_{d10} (°C)	Uptake (%)
	Theoretical data	Calculated data		
MT0	0	–	390	62.3
MT5	5	4.6	347	62.3
MT10	10	10.2	336	62.2
MT20	20	19.3	323	61.5
MT30	30	30.4	327	59.4
MT40	40	40.2	310	56.3
Pure TiO ₂	100	–	–	–

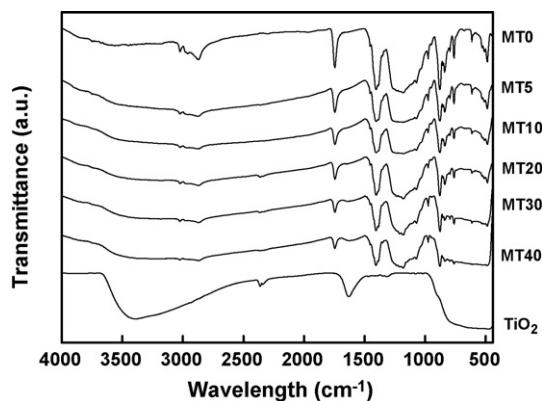


Fig. 2. Fourier transform infrared spectra of TiO₂ and porous membranes.

membranes towards a lower value is the result of the addition of TiO₂. The decrease in the thermal stability of porous membranes does not pose a limitation when using them as matrices for polymer electrolytes because the thermal stability at such high operating temperature is not necessary for the practical application of batteries.

The Fourier transform infrared (FT-IR) spectra of pure TiO₂ (100% anatase type) and porous membranes are shown in Fig. 2. The strong vibrational bands at 531, 766 and 976 cm⁻¹ are characteristic peaks of the α -phase PVdF crystals, and the bands at 484 and 840 cm⁻¹ correspond to γ - and β -phase PVdF crystals, respectively [16]. Moreover, the stretching mode vibration for carbonyl groups of P(EO-EC) at 1747 cm⁻¹ and the stretching mode vibration for the Ti–O band at 1640, 800 and 450 cm⁻¹ can be seen. In the case of pure TiO₂, the OH stretching vibration band is present at ca. 3400 cm⁻¹ due to the water molecules absorbed in TiO₂. Even though the intensity of the OH peak is more and more evident with increasing the TiO₂ content, it is still not so sufficiently noticeable to suggest that the water molecules absorbed in TiO₂ are completely excluded by the preparation conditions of porous membranes, namely, an ultralow moisture environment and prolonged vacuum drying at high temperature (above 100 °C). From Fig. 2, it is apparent that the peak intensities corresponding to polymer crystals disappear with increase in TiO₂ content, except for a small peak that is associated with the α -phase PVdF crystal at 976 cm⁻¹. These decreases and disappearances of peak intensities are considered to be attributed to the fact that the TiO₂ nanoparticles are well blended within the polymers, and this in turn confirms that the TiO₂ dispersion in porous membranes is well established.

The crystalline properties were also characterized by means of wide-angle X-ray diffraction (WAXRD) to confirm the change in the dominant crystal phase. The X-ray diffraction patterns of pure TiO₂ and porous membranes are presented in Fig. 3. It has been found [17] that some characteristic peaks due to α -phase crystals of PVdF are present at $2\theta \approx 17^\circ$, 19° and 38° together with the characteristic peak for γ -phase crystals of PVdF at $2\theta \approx 19^\circ$. The peak for the α -phase PVdF crystal observed at $2\theta \approx 38^\circ$ for MT0 disappears almost completely when P(EO-EC) is added. Anatase TiO₂ shows peaks at $2\theta \approx 26^\circ$ and 36° and these correspond to (1 0 1) and (0 0 4) planes. The

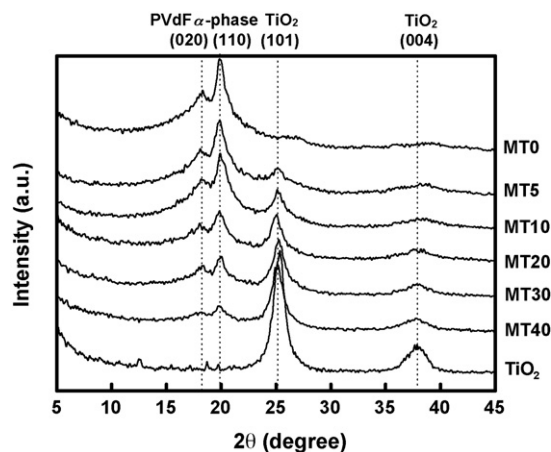


Fig. 3. Wide-angle X-ray diffraction patterns of TiO₂ and porous membranes.

peak intensities corresponding to PVdF crystals decrease with increase in TiO₂ content in porous membranes and almost disappear at 40 wt.% TiO₂ (i.e., MT40). Only a small peak remains and is identified as the α -phase, which agrees with the FT-IR data. Thus, the crystallinity reflected by the PVdF chain crystal decreases only gradually with increase in TiO₂ content.

3.2. Uptake and morphology of porous membranes

With respect to the pore-filling polymer electrolyte, the general understanding is that a higher uptake of a viscous electrolyte in the pores of a porous membrane leads to higher ionic conductivity. In the case of composite polymer electrolytes filled with organic solvents (also called plasticizers), the uptake values are usually greater than those in polymer electrolytes with no filler, and thus guarantees a higher ionic conductivity [18]. In this study, however, most of the TiO₂-filled porous membranes do not absorb viscous electrolyte to the same degree as that absorbed by the TiO₂-free porous membrane (MT0), as shown in Table 1. Moreover, the uptake of porous membranes is found to decrease slightly with increasing TiO₂ content and abruptly decreases above 20 wt.% TiO₂. This is probably due to difficult absorption of a viscous electrolyte into pores of TiO₂ nanoparticles compared with organic solvents. Also, as observed in the morphology of porous membranes (see below), the TiO₂ aggregation in samples with high TiO₂ content may be the main reason for the low uptake values.

Scanning electron micrographs of porous membrane surfaces with different TiO₂ contents are presented in Fig. 4. The images show relatively well-defined pore structures with pores of ca. 4–6 μm in size inside the membrane. At low TiO₂ loadings, it is clear that there is good dispersion of nanoparticles in the porous membranes. At higher TiO₂ loadings (≥ 30 wt.%), however, TiO₂ nanoparticles start to agglomerate. This accounts for the decrease in uptake of viscous electrolyte in the porous membranes. In order to confirm the presence and distribution of titanium in a porous membrane, energy dispersive spectroscopy (EDS) analysis was performed on the surface and cross-section of the MT10 sample. The images given in Fig. 5 show that there is a homogeneous distribution of TiO₂ throughout the surface

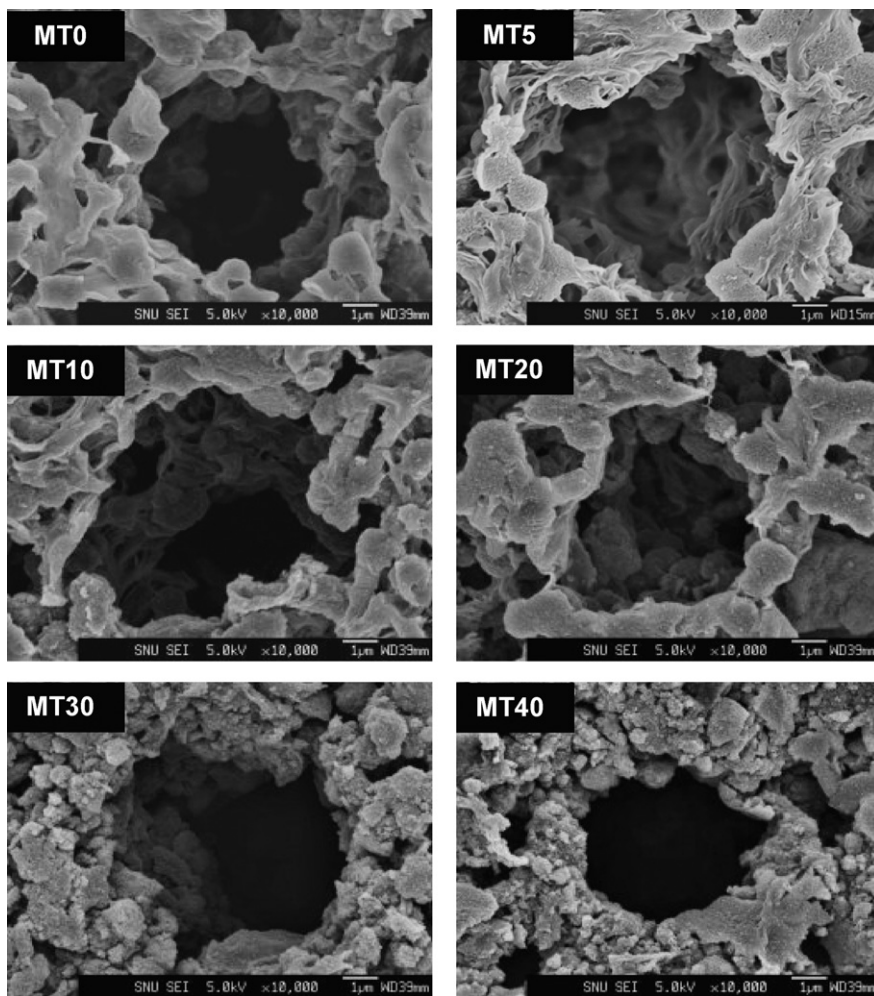


Fig. 4. Typical FE-SEM micrographs of surfaces of porous membranes.

and cross-section of the porous membrane. With increase of TiO_2 content in porous membranes, the titanium distribution gradually increases.

3.3. Mechanical properties of porous membranes

Tensile tests have generally been used to investigate the mechanical properties of polymer electrolytes. Because porous membranes play effective roles as matrices in polymer electrolytes, their mechanical properties are an important factor that must be considered in the battery manufacturing process. In this study, stress–strain measurements were taken on dry porous membranes. The curves for porous membranes with 0–40 wt.% TiO_2 are given in Fig. 6. The tensile strength increases up to a maximum value of 2.0 MPa and then markedly decreased with increase in TiO_2 content because excess TiO_2 (e.g., greater than 30 wt.%) might cause aggregation. This is consistent with the FE-SEM result that at high loading (≥ 30 wt.%) TiO_2 nanoparticles start agglomerating. On the other hand, the strain values slightly decrease up to 10 wt.% TiO_2 content and then decrease with increase in TiO_2 content. These results indicate that the addition of 10 wt.% TiO_2 has a positive effect on the mechanical properties of porous membranes because the tensile strength

of MT10 increases markedly, i.e., from 0.75 to 1.43 MPa without sacrificing its strain value. This increase in tensile strength is due to interactions between the carbonate and ether groups of P(EO-EC) and the hydroxyl group of TiO_2 .

From the above results, it can be concluded that the MT10 material is the most promising matrix in terms of mechanical properties as well as uptake of electrolyte. Thus, this material is chosen for evaluation tests.

3.4. Ionic conductivity of polymer electrolytes

The ionic conductivities of the polymer electrolytes were measured by means of an ac impedance analyzer. As mentioned above, MT10 was selected as a suitable porous membrane for the preparation of polymer electrolytes. Also, the Li-salt concentration was fixed at $1.5 \text{ mmol (g-P(EO-EC))}^{-1}$ based on the findings in previous studies [1,2]. Arrhenius plots of the polymer electrolytes are presented in Fig. 7. Interestingly, even though there is a slight curvature in some of the plots, all polymer electrolytes showed a linear enhancement of ionic conductivity when the temperature is increased. This means that the ion conduction mechanism of these polymer electrolytes is not due to the dynamic configuration of the polymer matrix but rather

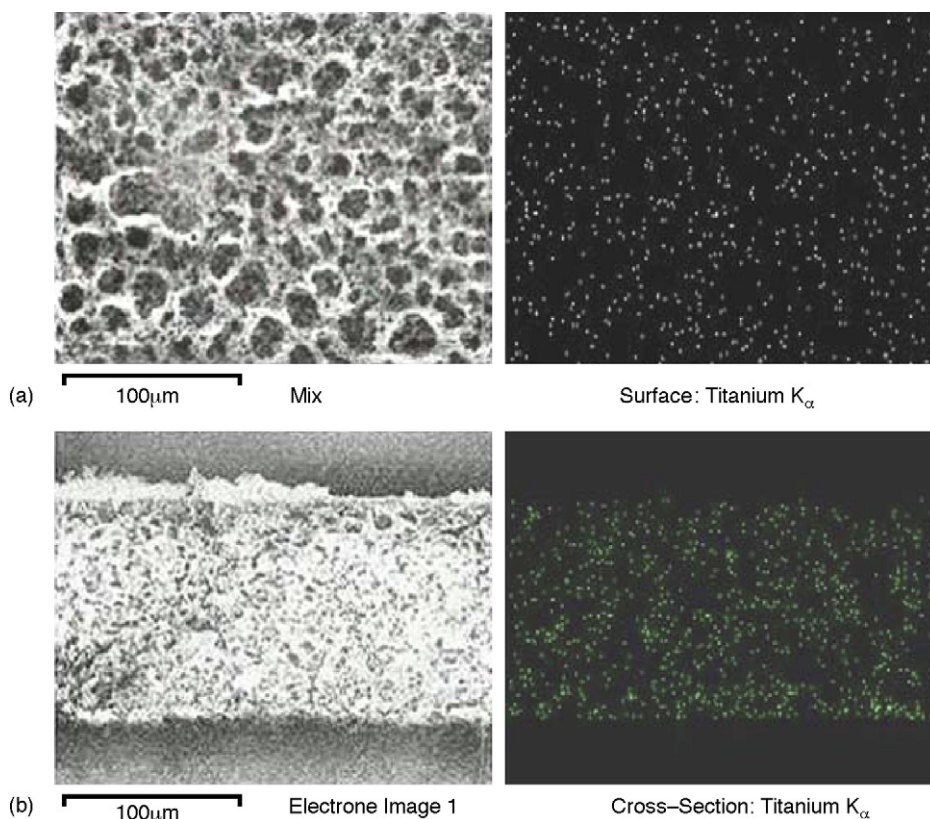


Fig. 5. Micrographs of (a) surface and (b) cross-section of MT10 measured using FE-SEM with EDS.

to the conduction path that is formed by filling the pores of a porous membrane with a viscous P(EO-EC)/LiCF₃SO₃/TiO₂ electrolyte.

On the other hand, as shown in Table 2, the ionic conductivity of polymer electrolyte increases up to 1.5 wt.% TiO₂ in a viscous electrolyte, and when the TiO₂ is added further the conductivity begins to decrease. This decrease is probably due to aggregation of TiO₂ nanoparticles. Thus, ET10-1.5 shows a maximum value of $5.1 \times 10^{-5} \text{ S cm}^{-1}$ at 25 °C. This is still lower than that of most gel systems, but nonetheless, it is noteworthy, that the value is higher than that for a LiCF₃SO₃-poly[oligo(ethylene glycol)-oxalate] complex [3], viz., ca. $8.0 \times 10^{-7} \text{ S cm}^{-1}$ at 25 °C and

for a LiCF₃SO₃-poly(methoxytriethyleneoxide)methylsiloxane complex [19], viz., ca. $1.2 \times 10^{-5} \text{ S cm}^{-1}$ at 30 °C, both of which are solvent-free polymer electrolytes based on an amorphous polymer of low molecular weight. This difference in conductivity is due to the pore-filling system prepared by filling the pores of a membrane with a viscous P(EO-EC)/LiCF₃SO₃/TiO₂ electrolyte, which plays an effective role as an ion conductor. The above value (i.e., $5.1 \times 10^{-5} \text{ S cm}^{-1}$) is also comparable with $3.2 \times 10^{-5} \text{ S cm}^{-1}$ of the TiO₂-free ET10-0. This implies that Li ions in a TiO₂-based electrolyte have higher mobility than those in a TiO₂-free electrolyte. In order to investigate the

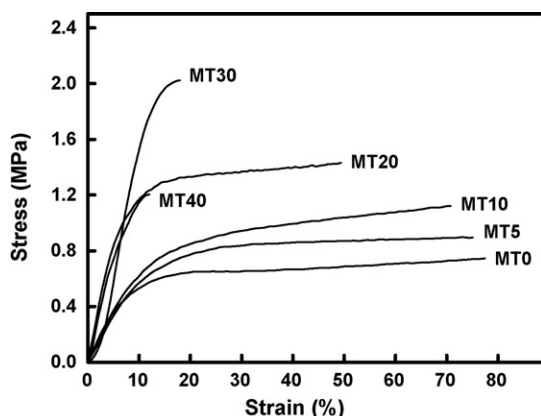


Fig. 6. Stress-strain curves of porous membranes.

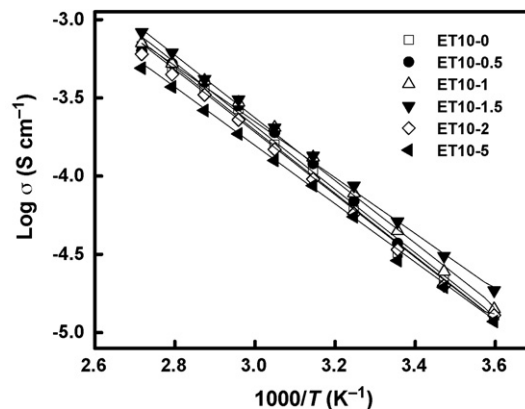


Fig. 7. Temperature dependence of ionic conductivity for polymer electrolytes with various TiO₂ contents. Data are fitted using the Arrhenius equation (solid lines).

Table 2
Ionic conductivity and activation energy data of polymer electrolytes

Sample	Ionic conductivity, σ (S cm ⁻¹)			Activation energy, E_a (kJ mol ⁻¹)
	At 25 °C	At 55 °C	At 85 °C	
ET10-0	3.2×10^{-5}	1.6×10^{-4}	4.9×10^{-4}	38.7
ET10-0.5	3.7×10^{-5}	1.9×10^{-4}	5.2×10^{-4}	38.9
ET10-1	4.7×10^{-5}	2.0×10^{-4}	5.3×10^{-4}	38.3
ET10-1.5	5.1×10^{-5}	2.1×10^{-4}	6.2×10^{-4}	34.3
ET10-2	3.4×10^{-5}	1.5×10^{-4}	4.5×10^{-4}	38.3
ET10-5	2.9×10^{-5}	1.3×10^{-4}	3.7×10^{-4}	38.9

role of TiO₂ nanoparticles, thermal analysis using a differential scanning calorimeter (DSC) was performed and is discussed below.

The slope of the Arrhenius plot is related to the activation energy, E_a , for ion transport by:

$$\sigma = \sigma_0 \exp\left(\frac{-E_a}{RT}\right) \quad (4)$$

where σ is the ionic conductivity; σ_0 is a constant; E_a is the activation energy; R is the gas constant; T is the temperature. The E_a values of all polymer electrolytes are in the range of 34–42 kJ mol⁻¹. Interestingly, ET10-1.5 has the lowest value of 34.3 kJ mol⁻¹, giving a low temperature dependence of conductivity. This underlines the fact that the polymer electrolyte with the highest conductivity can have the advantages of low temperature dependence and consequent uniform response over a wide temperature range in practical applications. The results are summarized in Table 2.

3.5. Thermal properties of viscous electrolytes

Typical DSC traces for pure P(EO-EC) and P(EO-EC)/LiCF₃SO₃/TiO₂ electrolytes with various TiO₂ contents are shown in Fig. 8. The neat P(EO-EC) (Fig. 8(a)) is in the amorphous state, since no melting transition is observed in the thermograms. When the Li-salt is added, the glass transition temperature, T_g , increased markedly, i.e., from -44.2

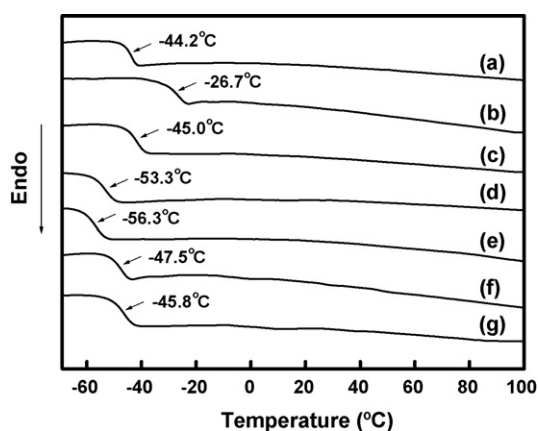


Fig. 8. DSC curves of (a) pure P(EO-EC) and P(EO-EC)/LiCF₃SO₃/TiO₂ electrolytes with (b) 0 wt.%, (c) 0.5 wt.%, (d) 1 wt.%, (e) 1.5 wt.%, (f) 2 wt.% and (g) 5 wt.% TiO₂.

to -26.7 °C, via the so-called ‘salt effect’. This behaviour is commonly observed in most polymer electrolytes formed by complexes of a Li-salt with a polyether-based polymer. It has been reported [3,20] that the increase in T_g is caused by interaction between lithium cations and the ether or carbonyl groups of polymers (i.e., oxide groups of polymers).

This interaction finally results in suppression of the freedom of polymer chain movement, to give a higher T_g . Then, after the addition of up to 1.5 wt.% TiO₂ in the viscous electrolyte, T_g tends to decrease. This decrease is believed to be associated with weakened interaction between Li⁺ ions and the oxide groups of P(EO-EC) by other interactions between hydroxyl groups of TiO₂ surface and oxide groups of P(EO-EC). This eventually leads to the improvement in the ionic conductivity because of the weakening of P(EO-EC) oxygen–lithium cation interactions, which allow relatively easy hopping of lithium cations. The T_g is lowered by the further addition of TiO₂. This is believed to be the result of TiO₂ aggregation, which leads to less P(EO-EC)–TiO₂ interactions.

4. Conclusions

In order to enhance the mechanical properties and ionic conductivity of pore-filling polymer electrolytes, TiO₂ nanoparticles have been added to both a porous membrane and a viscous electrolyte. It is confirmed that the crystallinity of the porous membrane decreases with the addition of TiO₂. TGA results show clearly that there are no significant differences in TiO₂ content between the theoretical and calculated data. This suggests that loss of TiO₂ nanoparticles does not occur during the washing process. The addition of 10 wt.% TiO₂ has a beneficial effect on the mechanical properties of the porous membranes because the tensile strength of MT10 increases markedly, i.e., from 0.75 to 1.43 MPa without any major decline in the strain value (i.e., from 77.5 to 70.8%). This is due to the interactions between the carbonate and ether groups of P(EO-EC) and the hydroxyl groups of TiO₂.

MT10 exhibits better performance (e.g., homogeneous distribution, high uptake of a viscous electrolyte) than the others and was therefore selected as an optimum matrix to prepare polymer electrolytes. The highest conductivity of 5.1×10^{-5} S cm⁻¹ at 25 °C is obtained for ET10-1.5 with 1.5 wt.% TiO₂ in a viscous electrolyte, compared with 3.2×10^{-5} S cm⁻¹ of ET10-0 without TiO₂. The glass transition temperature, T_g , is lowered by the addition of TiO₂ (up to 1.5 wt.% in a viscous electrolyte),

which is in good agreement with the conductivity result. This decrease in T_g is due to interaction between P(EO-EC) and TiO_2 , which weakens the interaction between the oxide groups of P(EO-EC) and lithium cations. On adding TiO_2 above 1.5 wt.%, T_g decreases as a result of agglomeration of TiO_2 . Based on the foregoing results, it is concluded that the addition of TiO_2 nanoparticles to both a porous membrane and a viscous electrolyte leads to enhancement of both the mechanical properties of porous membranes and the ionic conductivity of polymer electrolytes.

Acknowledgements

The authors are grateful to the Korea Science and Engineering Foundation (KOSEF) for the support of this study through the Hyperstructured Organic Materials Research Center (HOMRC).

References

- [1] J.-D. Jeon, B.-W. Cho, S.-Y. Kwak, J. Power Sources 143 (2005) 219–226.
- [2] J.-D. Jeon, S.-Y. Kwak, B.-W. Cho, J. Electrochem. Soc. 152 (2005) A1583–A1589.
- [3] W. Xu, J.-P. Belieres, C.A. Angell, Chem. Mater. 13 (2001) 575–580.
- [4] K.-S. Ji, H.-S. Moon, J.-W. Kim, J.-W. Park, J. Power Sources 117 (2003) 124–130.
- [5] G. Jiang, S. Maeda, Y. Saito, S. Tanase, T. Sakai, J. Electrochem. Soc. 152 (2005) A767–A773.
- [6] J.-H. Ahn, G.X. Wang, H.K. Liu, S.X. Dou, J. Power Sources 119–121 (2003) 422–426.
- [7] P.P. Prosini, S. Passerini, R. Vellone, W.H. Smyrl, J. Power Sources 75 (1998) 73–83.
- [8] G.B. Appetecchi, S. Scaccia, S. Passerini, J. Electrochem. Soc. 147 (2000) 4448–4452.
- [9] M.C. Borghini, M. Mastragostino, S. Passerini, B. Scrosati, J. Electrochem. Soc. 142 (1995) 2118–2121.
- [10] H.Y. Sun, H.J. Sohn, O. Yamamoto, Y. Takeda, N. Imanishi, J. Electrochem. Soc. 146 (1999) 1672–1676.
- [11] H.-T. Liao, C.-S. Wu, J. Polym. Sci. Part B: Polym. Phys. 42 (2004) 4272–4280.
- [12] P. Yang, D. Zhao, D.I. Margolese, B.F. Chmelka, G.D. Stucky, Nature 396 (1998) 152–155.
- [13] S.H. Chung, Y. Wang, L. Persi, F. Croce, S.G. Greenbaum, J. Power Sources 97–98 (2001) 644–648.
- [14] Y. Liu, J.Y. Lee, L. Hong, J. Power Sources 129 (2004) 303–311.
- [15] M. Zheng, M. Gu, Y. Jin, G. Jin, Mater. Sci. Eng. B77 (2000) 55–59.
- [16] M. Kobayashi, K. Tashiro, H. Tadokoro, Macromolecules 8 (1975) 158–171.
- [17] H.L. Marand, R.S. Stein, G.M. Stack, J. Polym. Sci. Part B: Polym. Phys. 26 (1988) 1361–1383.
- [18] K.M. Kim, N.-G. Park, K.S. Ryu, S.H. Chang, Polymer 43 (2002) 3951–3957.
- [19] E. Morales, J.L. Acosta, Electrochim. Acta 45 (1999) 1049–1056.
- [20] C.H. Park, D.W. Kim, J. Prakash, Y.-K. Sun, Solid State Ionics 159 (2003) 111–119.